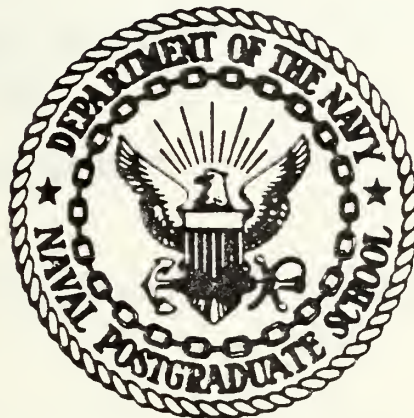


AN INVESTIGATION OF THE COMBUSTION
PROCESS IN SOLID FUEL RAMJETS

William Vernon Goodwin

NAVAL POSTGRADUATE SCHOOL

Monterey, California



THESIS

An Investigation of the Combustion Process
in Solid Fuel Ramjets

by

William Vernon Goodwin

June 1981

Thesis Advisor:

David W. Netzer

Approved for public release; distribution unlimited

T200043

REPORT DOCUMENTATION PAGE		READ INSTRUCTIONS BEFORE COMPLETING FORM
1. REPORT NUMBER	2. GOVT ACCESSION NO.	3. RECIPIENT'S CATALOG NUMBER
4. TITLE (and Subtitle) An Investigation of the Combustion Process In Solid Fuel Ramjets		5. TYPE OF REPORT & PERIOD COVERED Master's Thesis June 1981
7. AUTHOR(s) William Vernon Goodwin		6. PERFORMING ORG. REPORT NUMBER
9. PERFORMING ORGANIZATION NAME AND ADDRESS Naval Postgraduate School Monterey, California 93940		8. CONTRACT OR GRANT NUMBER(s)
11. CONTROLLING OFFICE NAME AND ADDRESS Naval Weapons Center China Lake, CA 93555		10. PROGRAM ELEMENT, PROJECT, TASK AREA & WORK UNIT NUMBERS N6053081WR30137
14. MONITORING AGENCY NAME & ADDRESS (if different from Controlling Office)		12. REPORT DATE June 1981
		13. NUMBER OF PAGES 58
		15. SECURITY CLASS. (of this report)
		15a. DECLASSIFICATION/DOWNGRADING SCHEDULE
16. DISTRIBUTION STATEMENT (of this Report) Approved for public release; distribution unlimited		
17. DISTRIBUTION STATEMENT (of the abstract entered in Block 20, if different from Report)		
18. SUPPLEMENTARY NOTES		
19. KEY WORDS (Continue on reverse side if necessary and identify by block number) Combustion Efficiencies, Regressions Rates, Temperature Profiles, Solid Fuel Ramjet,		
20. ABSTRACT (Continue on reverse side if necessary and identify by block number) An experimental investigation was conducted into four areas of the solid fuel ramjet combustion process: (1) the effects of near-wall turbulent mixing and equivalence ratio on combustion efficiency, (2) the effects of bypass air on combustion efficiency, (3) the combustion process in a cylindrically perforated fuel grain with a twin side-dump/dome configuration, and (4) the comparison of experimental radial temperature profiles to computer generated radial profiles. (continued)		

No. 20 (continued)

Polymethylmethacrylate fuel grains were burned in a ramjet motor on a thrust stand. Combustion efficiencies were determined and compared for different configurations. It was found to be insensitive to variations in the mixture ratio and to near-wall mixing. Bypass air was found to adversely affect the combustion efficiency both in stable and unstable combustion environments. The twin side-dump/dome configuration was unable to sustain combustion for all conditions investigated. Theoretical radial temperature profiles were found to have larger near wall gradients than were measured experimentally.

Approved for public release; distribution unlimited

An Investigation of the Combustion Process
in Solid Fuel Ramjets

by

William Vernon Goodwin
Lieutenant Commander, United States Navy
B.S., United States Naval Academy, 1972

Submitted in partial fulfillment of the
requirements for the degree of

MASTER OF SCIENCE IN ENGINEERING SCIENCE

from the

NAVAL POSTGRADUATE SCHOOL
June 1981

ABSTRACT

An experimental investigation was conducted into four areas of the solid fuel ramjet combustion process: (1) the effects of near-wall turbulent mixing and equivalence ratio on combustion efficiency, (2) the effects of bypass air on combustion efficiency, (3) the combustion process in a cylindrically perforated fuel grain with a twin side-dump/dome configuration, and (4) the comparison of experimental radial temperature profiles to computer generated radial profiles.

Polymethylmethacrylate fuel grains were burned in a ramjet motor on a thrust stand. Combustion efficiencies were determined and compared for different configurations. It was found to be insensitive to variations in the mixture ratio and to near-wall mixing. Bypass air was found to adversely affect the combustion efficiency both in stable and unstable combustion environments. The twin side-dump/dome configuration was unable to sustain combustion for all conditions investigated. Theoretical radial temperature profiles were found to have larger near wall gradients than were measured experimentally.

TABLE OF CONTENTS

I.	INTRODUCTION -----	13
II.	METHOD OF INVESTIGATION -----	16
III.	DESCRIPTION OF APPARATUS -----	18
	A. RAMJET MOTOR -----	18
	B. AIR SUPPLY AND CONTROL SYSTEM -----	19
	C. DATA ACQUISITION SYSTEM -----	19
IV.	EXPERIMENTAL PROCEDURES -----	21
	A. CALIBRATIONS -----	21
	B. DATA EXTRACTION -----	21
	C. REACTING FLOW EXPERIMENTS -----	22
V.	RESULTS AND DISCUSSION -----	27
	A. INTRODUCTION -----	27
	B. THE EFFECTS OF NEAR-WALL MIXING AND EQUIVALENCE RATIO ON COMBUSTION EFFICIENCY -----	27
	1. Cylindrically Perforated Fuel Grains of Varying Lengths Without Bypass -----	27
	2. Cylindrically Perforated Fuel Grains of Varying Lengths With Circumferential Grooves and Without Bypass -----	28
	C. THE EFFECTS OF BYPASS AIR ON COMBUSTION EFFICIENCY -----	29
	1. Cylindrically Perforated Fuel Grains of Varying Lengths With Bypass -----	29
	2. Cylindrically Perforated Fuel Grains Without Bypass and a Shortened Aft Chamber- -----	29
	3. Cylindrically Perforated Fuel Grains With Bypass and Choked Inlets -----	30

D.	THE COMBUSTION PROCESS IN A CYLINDRICALLY PERFORATED FUEL GRAIN WITH A TWIN SIDE-DUMP/ DOME CONFIGURATION -----	31
E.	THE EFFECT OF AIR FLOW RATE ON THE RADIAL TEMPERATURE PROFILE NEAR THE AFT END OF THE FUEL GRAIN -----	32
1.	Cylindrically Perforated Fuel Grain With Imbedded Thermocouples Without Bypass-----	33
2.	Cylindrically Perforated Fuel Grain With Imbedded Thermocouples with Bypass -----	35
3.	Comparison of Computer Model Temperature Profiles With Experimental Profiles -----	36
VI.	CONCLUSIONS AND RECOMMENDATIONS -----	43
	LIST OF REFERENCES -----	57
	INITIAL DISTRIBUTION LIST -----	58

LIST OF TABLES

Table	Page
I. Results of All Successful Experiments -----	38
II. Performance Summary for Cylindrically Perforated Fuel Grains Without Bypass -----	40
III. Performance Summary for Cylindrically Perforated Fuel Grains With Circumferential Grooves Without Bypass -----	40
IV. Performance Summary for Cylindrically Perforated Fuel Grains of Varying Lengths With Bypass -----	41
V. Performance Summary for Cylindrically Perforated Fuel Grains With Shortened Aft Mixing Chamber --	41
VI. Performance Summary for Cylindrically Perforated Fuel Grains With Bypass and Choked Inlets -----	42
VII. Air Flow and Inlet Size Summary for Cylindrically Perforated Fuel Grain With Twin Side-Dump/Dome Configuration -----	42

LIST OF FIGURES

Figure No.	Page
1. Schematic of Cylindrically Perforated Fuel Grain ---	44
2. Schematic of Cylindrically Perforated Fuel Grain With Circumferential Grooves -----	44
3. Photograph of Ramjet Motor Assembly with Shortened Aft Mixing Chamber -----	45
4. Schematic of Cylindrically Perforated Fuel Grain With Twin Side-Dump/Dome Inlets -----	46
5. Schematic of Cylindrically Perforated Fuel Grain With Imbedded Thermocouples -----	47
6. Schematic of Solid Fuel Ramjet Assembly -----	48
7. Photograph of Solid Fuel Ramjet Assembly -----	49
8. Schematic of Air Supply System -----	50
9. Combustion Efficiency vs. Mixture Ratio -----	51
10. Thermocouple Calibration Curves -----	52
11. Temperature vs. Time for Experiment No. 20 -----	53
12. Radial Temperature Profiles for Experiment No. 20 ---	54
13. Temperature vs. Time for Experiment No. 19 -----	55
14. Radial Temperature Profiles for Experiment No. 19 ---	56

SYMBOLS

A	area
A^*	nozzle throat area
f/a	fuel-air ratio
d	orifice diameter
D	diameter (pipe, fuel grain)
F	thrust
F_a	area factor for thermal expansion of steel
h_w	effective differential pressure
L	PMM fuel grain length
M	Mach number
\dot{m}	mass flow rate
P	pressure
P_t	stagnation pressure
R	gas constant
\dot{r}	fuel regression rate
r	radius
t_b	burn time
T	temperature
T_{ex}	experimental combustion stagnation temperature
T_{th}	theoretical combustion stagnation temperature
ΔW_f	weight change
Y	expansion factor
γ	ratio of specific heats
η	combustion efficiency

ρ density

ϕ equivalence ratio = $\frac{(f/a)}{(f/a)_{\text{stoichiometric}}}$

SUBSCRIPTS

a	air, ambient conditions
av	average
c	chamber
f	final
H	head
i	initial
p	primary
s	secondary
t	total

ACKNOWLEDGEMENT

I wish to acknowledge the help of Professor David Netzer who provided me help and assistance in completing this report. A very special thanks is also given to Mr. Uri Katz without whose guidance and assistance this project would not have been accomplished.

I. INTRODUCTION

Along with the increasing demands being placed on tactical missiles and concurrent improvements in warhead and guidance capabilities there has been a renewed interest in the development of the solid fuel ramjet propulsion system.

The distinguishing features of the solid fuel ramjet (SFRJ) are the absence of fuel tankage, fuel delivery and fuel control systems. The fuel is entirely packaged in the combustor. The SFRJ combines the inherent operational simplicity of a solid propellant, the potential loading efficiency of a solid fuel rocket motor and the performance of an airbreathing cycle [Ref. 1].

In order to be competitive with other types of modern propulsive systems the SFRJ must show that it has a stable and efficient combustion process. Furthermore, the combustion efficiency must be demonstrated over the expected operating envelope of altitudes and Mach numbers.

In the early 1970's the Chemical Systems Division of United Technologies (CSD) carried out studies dealing directly with SFRJ combustor development. Using both the by-pass and non by-pass configurations of the combustor a technology base was established. This technology base is most often characterized by fuel regression rates and by combustor efficiencies.

Investigations into the combustion behavior of the SFRJ have progressed steadily since 1973 at the Naval Postgraduate School. In 1980 Scott [Ref. 2] sought to relate the reacting and non-reacting flow characteristics of solid fuel ramjets. Results of Scott's work indicated that an increase in the near-wall turbulence intensity measured in non-reacting flow correlates with an increased fuel grain regression rate in the reacting environment. This in turn can affect the combustion efficiency, depending upon the value of the equivalence ratio.

This project continued the work begun by Scott. In this investigation an attempt was made to determine whether or not the combustion efficiency could be practically controlled by increased near wall turbulence mixing. Specifically, cylindrically perforated grains of varying lengths (in order to vary the fuel-air ratios from fuel lean to fuel rich) were to be hot fired and combustion efficiencies determined. The experiments were then to be repeated with circumferentially grooved grains, and the results compared to those of the ungrooved grains in order to determine if near-wall mixing is beneficial. If an effect could be demonstrated then the grooves would be varied in number and in size in an attempt to optimize their effect on combustion efficiency.

In a related area the project also considered the combustion process in a cylindrically perforated fuel grain

with a twin side dump/dome configuration. This configuration has the potential of maximizing the use of the space and volume constraints of the SFRJ.

In a further related area an attempt was made to obtain a better understanding of the effect of by-pass air on the combustion efficiency of the SFRJ. Experiments were to be performed with different combustor geometries and with various dump locations for by-pass air in order to see what effects these changes have on combustion efficiency.

Finally, the project sought to determine radial temperature profiles in the combustor near the aft end of the fuel grain for various air mass flow rates. These data were needed to provide information for the validation of an existing computer model for the SFRJ combustion process.

II. METHOD OF INVESTIGATION

Based on the work of Scott [Ref. 2], initial data collection consisted of selecting cylindrically perforated PMM grains (Fig. 1) of varying lengths and hot firing them. The varying lengths were chosen so that they produced air-to-fuel ratios that ranged from relatively lean to relatively rich. Combustion efficiencies of these grains were computed for both the non-bypass and the bypass configurations. The combustion efficiencies of these grains were then compared to the combustion efficiencies of cylindrically perforated grains of varying lengths that also had internal grooves machined into them (Fig. 2). The intention was to determine whether or not the combustion efficiency could be practically controlled by near-wall turbulence/mixing or if the dependence of the combustion efficiency on the fuel-to-air ratio was the overriding factor.

The next area of data collection consisted of hot firing a PMM grain in the non-bypass configuration but having a much shorter aft mixing chamber (Fig. 3). The purpose was to determine what percentage of the combustion occurred aft of the fuel grain.

Following these experiments the hot firing of a cylindrically perforated fuel grain with a twin side-dump/flat dome configuration (Fig. 4) was attempted. The dome length

was 2.1 inches and the dump diameters were 0.354 inches. The twin dump configurations had never been successfully fired [Ref. 2].

Finally, in an attempt to determine the radial temperature distribution in the fuel rich region between the wall and flame, a cylindrically perforated fuel grain was prepared with a series of eight thermocouples imbedded in it near the aft end (Fig. 5). Two grains of this configuration were then hot fired.

III. DESCRIPTION OF APPARATUS

A. RAMJET MOTOR

The ramjet motor assembly used in the experiments is shown in figure 1. The primary parts of the assembly included the head-end section, the step insert section, the fuel grain and the aft mixing chamber.

Primary air-flow is introduced into the head-end assembly through two openings as shown in figure 1. Also located in the head-end assembly were ports for the introduction of the ignition fuel and the igniter torch. Attached to the head-end assembly was a pressure tap which allowed measurement of the inlet pressure.

The step insert section permitted variations in the size of the inlet diameter.

The mid-section of the motor was the PMM grain. "O" rings located in the head-end assembly and in the aft mixing chamber provided a tight seal for the entire assembly. Once in place the fuel grain was secured in position by three threaded rods and nuts.

The final part of the motor was the aft mixing chamber. Here the bypass air could be introduced at various axial locations or, alternatively, the chamber could be configured for non-bypass experiments by plugging the bypass air ports. The aft section of the mixing chamber was the ramjet nozzle.

For all hot firings a converging nozzle with a 0.75 inch throat diameter was used. Combustor pressure was measured near the aft end of the mixing chamber. An orifice was used at the aft end of the fuel grain to maintain a fixed area ratio between the fuel port and the aft mixing chamber.

The entire ramjet motor assembly is shown in figure 7.

B. AIR SUPPLY AND CONTROL SYSTEM

The air supply system used for the experiments is shown in figure 8. The source of the air was a Pennsylvania Low Pressure Air Compressor which could supply air up to 150 psi. From the compressor the air was fed into a large reservoir tank. A fourteen inch gate valve controlled the flow of air from the reservoir tank to the primary and secondary flow pipes located just upstream of the ramjet motor assembly. Standard ASME orifice flow meters were used to measure the flow rates of the air into the motor for both the primary and secondary air. Two manually operated gate valves, one in the primary air line and one in the secondary air line, were used to establish the required flow rates to the motor. When required, the primary air could be vented to the atmosphere instead of through the motor by the use of two pneumatically operated ball valves.

C. DATA ACQUISITION SYSTEM

Six pressure transducers were located in the system in order to sense both primary and secondary line and differential

pressures and also the head and chamber pressures of the ramjet motor. Thrust measurements were made with a strain gage load cell. All of these measuring devices had their outputs recorded on a Honeywell Visicorder.

When required, temperature profile measurements were accomplished by attaching the thermocouples embedded in the fuel grain directly to a second Visicorder. Air temperatures were measured with thermocouples and recorded on a strip chart.

A five hertz signal from a frequency generator was used to provide an accurate time reference on the Visicorder.

Data obtained from the Visicorder and strip chart were used to determine air flow rates, fuel-to-air ratios and average fuel regression rates. Combustion efficiencies were calculated using the equilibrium gas properties and temperatures generated by use of the NWC PEPCODE computer program (run on the IBM-3033 system computer at the Naval Postgraduate School).

IV. EXPERIMENTAL PROCEDURES

A. CALIBRATIONS

Prior to and following each set of hot firings the pressure transducers (including Kistler transducers for monitoring combustion pressure oscillations) and thrust pickup were calibrated over the expected ranges of pressures and thrusts.

B. DATA EXTRACTION

The Visicorder traces were used to determine all pressure and thrust readings for a given experiment. Using the time signal on the trace as the basis for determining the "middle" of the experiment, a line was then drawn vertically through this "middle" position. Then, by measuring from the equivalent zero location for any one of the desired parameters (thrust, chamber pressure, etc.) to the corresponding steady-state location on the vertical line, a characteristic length was determined. This characteristic length was then multiplied by the corresponding calibration value. The figure obtained was the numerical value (adjusted to absolute pressure as required) used in all subsequent calculations.

The numerical values obtained by the above method of data extraction from the Visicorder traces were verified by a comparison with numerical values extracted from the traces with a compensating polar planimeter. The planimeter was

used to measure the area under each trace. The measured area was divided by the measured length of that trace. This resulted in an average trace height. The comparison of the numerical values obtained by each method showed little, if any, difference.

C. REACTING FLOW EXPERIMENTS

Following the calibration and the installation of the fuel grain into the motor assembly, the mass flow rate of air was manually set according to the particular value required for a given experiment. Typically, these values were 0.2 lbm/sec for the primary air in a non-bypass experiment and 0.1 lbm/sec for both the primary and secondary air in a bypass configured experiment. The actual values were established by setting the correct differential pressures across the orifices in the primary and secondary air lines.

The equation used to determine the mass flow rate of air was [Ref. 3]:

$$\dot{m}(\text{lbm/sec}) = 0.099702 K F_a d^2 Y \sqrt{\rho h_w} \quad (1)$$

where

$$K = \frac{C}{\sqrt{1-\beta^4}}$$

C = orifice discharge coefficient

β = d/D (orifice diameter/pipe diameter)

F_a = area factor for thermal expansion of steel

Y = expansion factor = $1 - (.41 + .35\beta^4) \frac{\Delta P}{P_Y}$

P = line pressure (psia)

γ = ratio of the specific heats of the gas

ρ = density of the gas (lbm/cu.ft.)

h_w = effective differential pressure
(in. of water at 68°F)

ΔP = differential pressure (psi)

Typically the ignition sequence was started by setting the desired air-flow rate(s), and then activating the ignition switch. Activation of the ignition switch caused ethylene gas to be injected into the forward part of the fuel grain along with the primary air flow. The resulting mixture was then ignited by an oxygen-ethylene torch whose flame came out of the surface of the step- inlet. A successful ignition usually lasted between two and three seconds.

The majority of the reacting flow experiments lasted approximately 45 seconds. At the completion of the experiment the loss in fuel grain weight was recorded.

Following data extraction from the Visicorder traces, hand calculations were performed in order to determine the desired parameters from each individual experiment.

The mass flow rate of air was determined from equation (1) using the actual recorded values of P and ΔP .

The mass flow rate of fuel was determined by weighing the fuel grain before and after the experiment and dividing by the time duration of the experiment (adjusted for any ignition delay).

Following determination of the flow rates the theoretical adiabatic combustion stagnation temperature T_{th} was determined from the known fuel-to-air ratio and combustion pressure.

The average fuel regression rate was also determined based on the change from the initial to final average diameter. The initial average diameter was measured with a snap gage and micrometer. The final average diameter was determined based on weight loss by using the following equation:

$$Df_{av} = \sqrt{\frac{4(\Delta W)}{\pi L \rho} + Di_{av}^2} \quad (2)$$

where

ΔW = weight change in pounds

L = length of the fuel grain in inches

ρ = density of PMM (0.0426 lbm/cubic inch)

Di_{av} = initial average diameter in inches

The average fuel regression rate was then computed using

$$\dot{r}_{av} = \frac{Df_{av} - Di_{av}}{2 t_b} \quad (3)$$

where

t_b = duration of the experiment in seconds
adjusted for ignition delay

Experimental combustion stagnation temperatures (T_{ex}) were calculated based on the static pressure in the combustion

chamber and the measured flow rates. The one dimensional continuity equation for choked flow through a converging nozzle was expressed in terms of the combustion chamber stagnation pressure (P) [Ref. 4].

$$\dot{m}_t = \frac{P_t A^* \sqrt{g}}{\sqrt{R T_{ex}}} \left[\gamma \left(\frac{2}{\gamma+1} \right)^{\frac{\gamma+1}{\gamma-1}} \right]^{\frac{1}{2}} \quad (4)$$

From this expression the stagnation temperature T was found.

$$T_{ex} = \left[\frac{P_t A^*}{\dot{m}_t} \right]^2 \left[\frac{g\gamma}{R} \left(\frac{2}{\gamma+1} \right)^{\frac{\gamma+1}{\gamma-1}} \right] \quad (5)$$

Measurements were made of chamber static pressure (P_c) instead of chamber stagnation pressure (P_t). Since the flow was isentropic the relationship between P_c and P_t can be expressed as

$$\frac{P_t}{P_c} = \left(1 + \frac{\gamma-1}{2} M^2 \right)^{\frac{\gamma}{\gamma-1}} \quad (6)$$

It was found that the Mach number M was typically less than 0.07 so that P_t could be set equal to P_c with less than 0.5% error. The values of γ and R used in equation (5) were the equilibrium values obtained using the NWC PEPCODE computer program.

Once T_{ex} and T_{th} were determined the combustion efficiency η was calculated using

$$\eta = \frac{T_{ex} - T_a}{T_{th} - T_a} \quad (7)$$

where

T_a was the inlet air temperature recorded on the strip chart.

V. RESULTS AND DISCUSSION

A. INTRODUCTION

In this chapter the results of each of the four areas of investigation are discussed. A total of 21 experiments were attempted, of which 20 were successful in that combustion was sustained. The results of these experiments are contained in Table I.

B. THE EFFECTS OF NEAR-WALL TURBULENT MIXING AND EQUIVALENCE RATIO ON COMBUSTION EFFICIENCY

In this area of investigation grain length was varied to effect changes in equivalence ratio and circumferential grooves were used to enhance near wall mixing.

1. Cylindrically Perforated Fuel Grains of Varying Lengths Without Bypass

Table II presents the combustion efficiencies of the cylindrically perforated fuel grains for experiments 1 through 4. This Table shows that for the non-bypass configuration with the mixture ratio varied (a result of varying the fuel grain lengths), there was no significant change in the combustion efficiency.

The results also indicate that, for PMM fuel, efficiencies of approximately 100% are consistently achieved regardless of the mixture ratio. Figure 9 is a graph of combustion efficiency vs. mixture ratio for these four experiments.

These results do not agree with the tentative conclusions arrived at by Scott [Ref. 2] who surmised that the combustion efficiency appeared to be a strong function of the mixture ratio with the maximum occurring near stoichiometric. However, that opinion was based upon very limited test results with fixed grain lengths.

2. Cylindrically Perforated Fuel Grains of Varying Lengths With Circumferential Grooves and Without Bypass

Table III presents the combustion efficiencies of experiments 9 and 10. This Table shows that a grooved grain with a similar length to that of a non-grooved grain had the effect of increasing the fuel regression rate (and therefore, the equivalence ratio). This could be beneficial for a system that requires a high regression rate but is limited in fuel grain length. However, the grooves did not increase or decrease the combustion efficiency (which was still 100% (Fig. 9)). In summary, near-wall mixing merely changed the equivalence ratio but did not change the essentially 100% combustion efficiency that was attained in the nominal configuration. Metochianakis [Ref. 5] has previously found that near wall mixing decreased combustion efficiency for HTPB fuels. That fuel does not have 100% combustion efficiency and η varies with ϕ .

C. THE EFFECTS OF BYPASS AIR ON COMBUSTION EFFICIENCY

In this second area of investigation three different experimental configurations were employed in order to determine the effect that bypass air has on the combustion efficiency of PMM.

1. Cylindrically Perforated Fuel Grains of Varying Lengths With Bypass

Table IV presents the performance summaries for experiments 5, 6, 7, 8, 11, 12, and 13. For the bypass configuration the combustion efficiencies were 22% to 28% lower than the combustion efficiencies of the non-bypass configured fuel grains (Fig. 9). The Table also shows that the combustion efficiencies were again insensitive to changes in the mixture ratio.

2. Cylindrically Perforated Fuel Grains Without Bypass and a Shortened Aft Mixing Chamber

The decrease in combustion efficiency noted above can result from the bypass air quenching the reaction in the aft mixing chamber and/or by affecting changes upstream within the fuel grain. In order to clarify this behavior, tests were conducted without bypass with a shortened aft mixing chamber. Table V contains the combustion efficiencies for the fuel grains from experiments 17 and 18. Experiment 18 used the same fuel grain that was used in experiment 17. With a much shorter aft mixing chamber (approximately 88% less volume than all previous runs, $L/D = .35$) there was a 7-8% loss in combustion efficiency when compared to

similar non-bypass configured grains with a full sized mixing chamber, (Fig. 9). These results indicate that approximately 7-8% of the combustion process takes place in the full sized aft mixing chamber ($L/D = 2.93$) without bypass. Assuming a similar behavior with bypass, the remaining 15-20% loss in efficiency when bypass was used apparently resulted from changes in the combustion process within the fuel grain.

3. Cylindrically Perforated Fuel Grains With Bypass and Choked Inlets

In a concurrent and related area of research, pressure oscillations (instabilities in the combustion process) were observed to be occurring in the experiments with the bypass configured fuel grains. In an effort to isolate the source of the instabilities both the primary and bypass air flows were choked at the motor inlets for experiments 14, 15 and 16. Table VI presents the performance summaries for these three experiments. The results indicated that the choking of the inlets did enable the combustion to occur under stable conditions. Figure 9 further shows that the combustion efficiency for these three experiments increased 15-20% over the bypass configured experiments with combustion instabilities. This was a return to the efficiency level attained without bypass but with the shortened aft mixing chamber configuration. These results indicate that, even though the bypass configuration can be

made to operate with stable combustion, the bypass air still adversely affected 7 to 8 percent of the combustion process; most probably by quenching the combustion process occurring in the aft mixing chamber. Apparently, the unburned hydrocarbons/carbon leaving the fuel grain burn most efficiently for PMM fuel when allowed to react more slowly in the aft mixing chamber.

D. THE COMBUSTION PROCESS IN A CYLINDRICALLY PERFORATED FUEL GRAIN WITH A TWIN SIDE-DUMP/DOME CONFIGURATION

In an effort to attain sustained combustion in a dome type configured fuel grain a modification to a previously configured [Ref. 2] dome type grain was made. This modification consisted of introducing primary air into the dome area of the grain through two dump injector ports instead of a single dump. In addition, each injection port was axially offset and inclined at an angle of 75 degrees to the centerline in the transverse plane of the grain. In order to insure that a swirl pattern would develop in the grain, the ports were further inclined 15 degrees in the longitudinal plane.

Three attempts to ignite this fuel grain proved to be unsuccessful. Each attempt represented a different mass flow rate of air. Following these attempts a circular disk of HTPB fuel (.25 in thick and 1.5 in. in diameter) was attached to the head of the dome. This was done in an effort to assist in the development of a sustained combustion

because HTPB has a higher regression rate than PMM. This configuration also proved to be unsuccessful in three attempts at ignition, again with varied mass flow rates. Table VI summarizes these attempts.

At the present time it is not known why combustion can not be sustained in this particular configuration.

E. THE EFFECT OF AIR FLOW RATE ON THE RADIAL TEMPERATURE PROFILE NEAR THE AFT END OF THE FUEL GRAIN

In this last area of investigation two experiments (19 and 20) were performed in order to obtain two different radial temperature profiles near the aft end of the fuel grain for two different air flow rates. The intent was to obtain experimental profiles and compare them with computer generated profiles that are in part dependent upon air flow rate as a data input. The comparison could then be used to assist in the validation of the computer model.

Two fuel grains were identically prepared with eight thermocouples imbedded one inch from the aft end of the grain. All of the thermocouples used were of the CHROMEL-ALUMEL type. Four of the eight thermocouples used 36 gage wire while the remaining four were 30 gage.

The four thermocouples of each size were imbedded to a distance of .02 in., .10 in., .18 in., and .25 in. from the inside grain wall. The thermocouples were also spaced 45 degrees apart from each other. Figure 5 is a sketch of

this configuration. It was hoped that with this arrangement the small gage thermocouples would provide a faster response time to temperature changes, while being complemented by the heavier gage thermocouples which would last longer in the expected high temperature, high velocity flow region.

1. Cylindrically Perforated Fuel Grain With Imbedded Thermocouples Without Bypass

This particular configuration was chosen for experiment No. 20 to provide the desired initial air flow rate of .20 lbm/sec. The voltage signals obtained from the thermocouples were input directly into a Visicorder. The traces obtained were then used with previously obtained calibration curves. The calibration curves (for both gages of thermocouples) were necessary since the experiments were conducted without the use of an ice bath or other type of reference junction. The calibration consisted of using an oxy-acetylene torch as a heat source for the thermocouples that were simultaneously being referenced to an electronic ice point. By measuring the temperature induced voltages on a digital volt meter the deflections on the Visicorder traces could be related to the temperature induced voltages. Figure 10 is a plot of this relationship for both types of thermocouples. The data extraction method used consisted of measuring the deflection distance from the Visicorder trace, entering the calibration curve with the distance and obtaining a corresponding voltage which was then used with tables that

relate the induced thermocouple voltage to the actual temperature being sensed by the thermocouple (uncorrected for radiation heating). Figure 11 is a graph of temperature vs. time for seven of the eight thermocouples used in experiment 20 (one small thermocouple showed no response). This graph clearly shows the similarities in the response times of each of the thermocouples to the increasing temperature as the fuel grain burned. This indicates that a uniform, axisymmetric flame boundary existed at this particular location in the fuel grain.

The actual average regression rate for this experiment was determined to be .0063 in/sec, based on the measured weight loss and previous experiments using the same configuration. Using this regression rate and the information from figure 11, a temperature vs. distance profile was produced as shown in figure 12. This graph shows the similarities in each of the profiles for the four heavy gage thermocouples. The graph represents the temperature profiles as they occurred in the fuel grain if the ordinate of the graph is located as shown. This would seemingly contradict, however, the knowledge that the surface temperature of burning PMM is approximately 600 degrees Kelvin. In order to take this into account the profiles need to be shifted either to the left or to the right within a range of .030 inches depending upon the thermocouple. Several experimental conditions affected

the profiles. The leveling off of the temperature occurred because the thermocouples bent over when they lost strength as they approached the flame. Each thermocouple also generated near-wall mixing and increased the local fuel regression rate. This, in turn, could reduce the local temperature because of the more fuel rich condition that was generated.

2. Cylindrically Perforated Fuel Grain With Imbedded Thermocouples With Bypass

This configuration change from experiment 20 was made for experiment 19 so that a lower air flow velocity in the fuel port could be achieved while still maintaining a choked exhaust nozzle. However, as discussed above, bypass air may affect the temperature profile within the fuel port. To minimize this effect the motor air inlets were operated in a choked condition.

Figure 13 shows the temperature vs. time profiles for six of the eight thermocouples in this experiment. Two of the thermocouples were never exposed to the flame due to the lower regression rate, a characteristic of the bypass configuration. Again there were similarities between all of the profiles, indicating the same conclusions drawn from experiment 20.

For this experiment the average regression rate was determined to be 0.0043 in./sec based on the measured weight loss and previous experiments using the same

configuration. Figure 14 is a plot of temperature vs. distance based on this regression rate. This graph shows an even better agreement between the profiles obtained with the heavy gage thermocouples than in experiment 20. As in experiment 20, in order to bring these profiles to a position that would agree with a 600 degree Kelvin surface temperature a shift to the left of from .0225 to .0274 inch in the profile would be required.

3. Comparison of Computer Model Temperature Profiles With Experimental Profiles

Using the primary air mass flow rate, the chamber pressure and the temperature of the inlet air as inputs to the computer program, temperature vs. distance profiles were predicted as shown in figures 12 and 14 as the dashed lines. The dashed line in figure 14 is based on the primary mass flow rate of air used in experiment 19 (.098 lbm/sec). The solid lines in figure 14 represent experimental profiles for experiment 19. The comparison shows that for the range of temperatures between 600 and 1000 degrees the profiles were similar. However, going beyond 1000 degrees there was a marked difference between the profiles. This difference is probably due to the fact that the thermocouples have by this time bent over and/or burned out, making them incapable of measuring the higher temperatures encountered. Since the computer model predicts temperatures of over 2500 degrees it would not be correct to make any further comparisons based on the available experimental data.

The dashed line in figure 12 is based on the mass flow rate of air used in experiment 20 (.194 lbm/sec). Upon comparison it can be seen that there was even less agreement between profiles than in the previous experiment with a lower air mass flow rate. Again, this could be attributed to the fact that the thermocouples have ceased to function at a much lower temperature (approximately 1500 degrees) than that which the computer model used as its final data point (approximately 2900 degrees).

Comparison between the theoretical and experimental profiles indicates that the computer model gives a steeper gradient for both the high and low air flow rates than those that actually occurred in the experiment.

The computer model also predicts a steeper gradient for the higher flow rate, but the experimental results indicate nearly identical gradients for both flow rates.

Table. I
Results of All Successful Experiments

Experiment No.	1	2	3	4	5	6	7	8	9
Config. *	NBP	NBP	NBP	NBP	BP	BP	BP	BP	NBP - Grooved
L (in)	12	14	16	18	14	18	22	24	8
ΔW_f (lbm)	.905	1.105	1.138	1.311	1.026	1.042	1.519	1.674	.722
\dot{m}_p (lbm/sec)	.204	.194	.199	.205	.097	.101	.101	.103	.201
\dot{m}_s (lbm/sec)	0	0	0	.0	.088	.091	.091	.092	0
m_t (lbm/sec)	.223	.214	.222	.231	.206	.214	.223	.226	.216
t_b (sec)	48.2	52.6	48.4	50	50.7	47.7	49.1	53.5	48
Di (in)	1.507	1.505	1.506	1.504	1.505	1.504	1.517	1.521	1.5
\dot{r}_{av} (in/sec)	.0064	.0057	.0061	.0060	.0059	.0052	.0058	.0054	.0074
f/a	.089	.102	.118	.127	.109	.114	.161	.160	.075
ϕ	.742	.908	.983	1.06	.909	.948	1.34	1.34	.624
$T_{ex}^{(OR)}$	3609	419	4092	4270	2889	3230	3393	3052	3171
F (lb _f)	23.22	25.80	29.67	29.67	22.90	24.20	26.87	32.70	21.45
η	1.02	1.06	0.99	1.03	0.82	0.79	0.93	0.82	1.00
Pc (psia)	58.9	60.9	63.7	66.5	48.3	53.5	57.12	55	53.5
P_H (psia)	67.6	66.9	69.9	73.3	51.1	56.9	61.6	60.3	62.3

*NBP = Non-Bypass

BP = Bypass

SHT MIX CHM = Short Mixing Chamber (Fig. 3)

Grooved = Circumferential Grooves (Fig. 2)

Table I (continued)

Experiment No.	10	11	12	13	14	15	16	17	18	19	20
Config.	NBP grooved		BP	BP	BP	BP	BP	NBP SHT MIX CHM	NBP SHT MIX CHM	BP w/ Thermo Couples	NBP Thermo Couples
L (in)	11	21	20	19	14	14	14	14	14	12	12
ΔW_f (lbm)	1.126	1.546	1.20	1.122	.543	.755	.419	.987	.642	.701	1.025
\dot{m}_p (lbm/sec)	.199	.103	.102	.098	.101	.100	.099	.197	.193	.098	.194
\dot{m}_s (lbm/sec)	0	.096	.091	.093	.092	.094	.095	0	0	.086	0
\dot{m}_t (lbm/sec)	.225	.227	.217	.216	.211	.209	.210	.218	.217	.196	.214
tb (sec)	48	55.04	50.4	46	29.8	49.4	27	47.1	26.3	57.1	50.65
Di (in)	1.5	1.503	1.51	1.51	2.11	1.51	1.97	1.50	2.09	1.51	1.51
\dot{r}_{av} (in/sec)	.0083	.0055	.0051	.0054	.0043	.0047	.0039	.0062	.0058	.0043	.0067
f/a	.118	.141	.123	.128	.094	.079	.080	.106	.126	.067	.104
ϕ	.983	1.17	1.03	1.06	.79	.65	.67	.88	1.05	.56	.87
T_{ex} (°R)	4093	3223	3308	3162	3447	3135	3321	3773	4055	2806	3777
F(lbf)	27.3	24.2	25.6	24.3	23.1	21.1	23.8	27.7	27.7	19.7	22.9
η	.99	.76	.76	.73	.93	.95	1.00	.94	.97	.94	.97
Pc (psia)	62.6	56.7	54.9	53.4	54.6	51.5	53.2	58.9	60.9	45.7	57.9
P _H (psia)	70.6	61.9	59.7	57.4	56.6	57.3	55.5	66.8	68.8	48.1	65.5

Table II

Performance Summary for Cylindrically
Perforated Fuel Grains Without Bypass

Test No.	L(in)	ϕ	η	\dot{r} (in/sec)
1	12	0.743	1.02	.0064
2	14	0.908	1.06	.0057
3	16	0.983	0.99	.0061
4	18	1.060	1.03	.0060

Table III

Performance Summary for Cylindrically Perforated Fuel
Grains With Circumferential Grooves Without Bypass

Test No.	L(in)	ϕ	η	\dot{r} (in/sec)
9	8	.624	1.00	.0074
10	11	.983	0.99	.0083

Table IV

Performance Summary for Cylindrically Perforated
Fuel Grains of Varying Lengths With Bypass

Test No.	L(in)	ϕ	η	\dot{r} (in/sec)
5	14	.91	.82	.0059
6	18	.948	.79	.0052
7	22	1.34	.93	.0058
8	24	1.34	.82	.0054
11	21	1.17	.76	.0055
12	20	1.03	.76	.0051
13	19	1.06	.73	.0054

Table V

Performance Summary for Cylindrically Perforated
Fuel Grains With Shortened Aft Mixing Chamber

Test No.	L(in)	ϕ	η	\dot{r} (in/sec)
17	14	.886	.94	.0062
18	14	1.05	.97	.0058

Table VI

Performance Summary for Cylindrically Perforated
Fuel Grains With Bypass and Choked Inlets

Test No.	L(in)	ϕ	η	\dot{r} (in/sec)
14*	14	.79	.93	.0043
15	14	.65	.95	.0047
16**	14	.68	1.00	.0039

* reused grain no. 5

** reused grain no. 15

Table VII

Air Flow and Inlet Size Summary for Cylindrically Perforated
Fuel Grain With Twin Side-Dump/Dome Configuration

Dd (in)	.354	.354	.354
Ld (in)	2.1	2.1	2.1
m (lbm/sec)	.15	.20	.25

VI. CONCLUSIONS AND RECOMMENDATIONS

Fuel grains of varying lengths along with fuel grains with circumferential grooves were tested in order to isolate the effects of mixture ratio and near-wall mixing on combustion efficiency. Efficiency did not vary with equivalence ratio. Near-wall mixing increased regression rate but did not increase efficiency. Since PMM burns essentially with 100% efficiency in all non-bypass configurations, other types of hydrocarbon based fuels should be used to study these effects.

Bypass air adversely affects the combustion efficiency when PMM fuel grains were used. The effect was greater when combustion pressure oscillations were present. It is recommended that further research be directed to the localization and cause of the combustion pressure oscillations.

The inability of the twin side-dump/dome configuration to sustain combustion still warrants further investigation. Possibly a fuel with even a higher rate of regression than HTPB could be used in the dome to stabilize the flame.

Finally, in order to obtain a better range in the experimental radial temperature profiles it is recommended that a probe be used instead of imbedded thermocouples to measure the flame temperatures. This could insure that experimental temperatures and theoretical temperatures would have a more meaningful comparison.

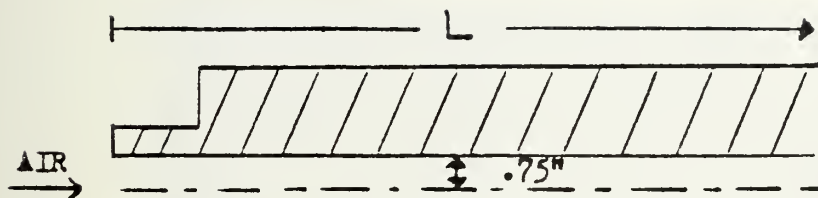


Figure 1. Schematic of Cylindrically Perforated Fuel Grain

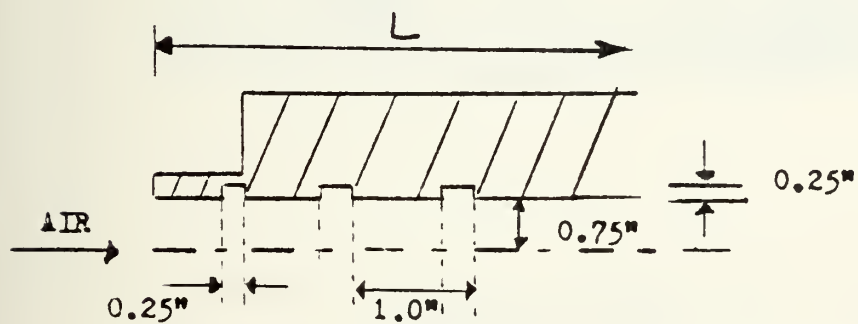


Figure 2. Schematic of Cylindrically Perforated Fuel Grain with Circumferential Grooves

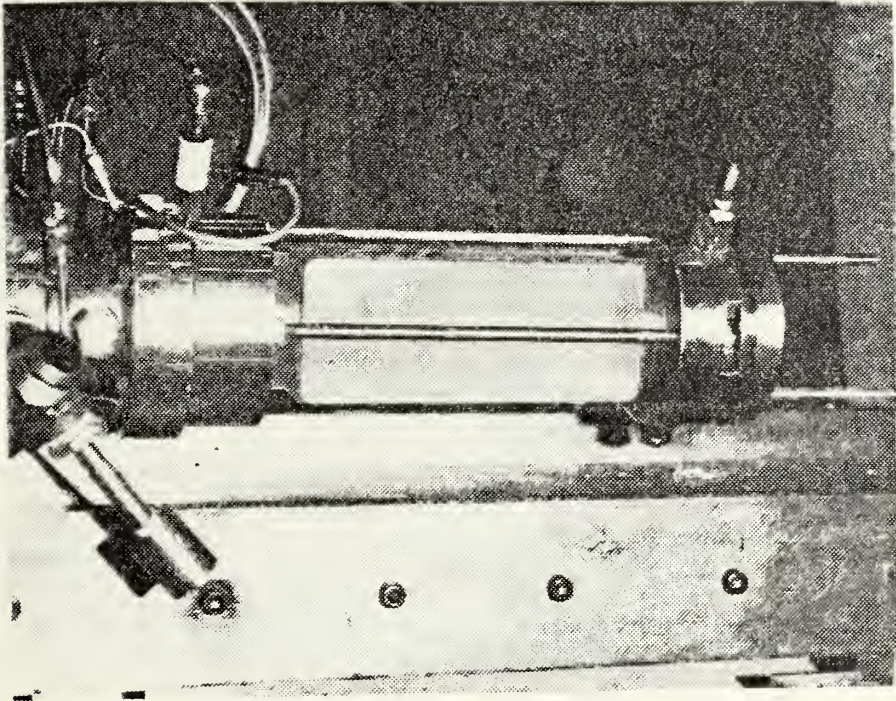
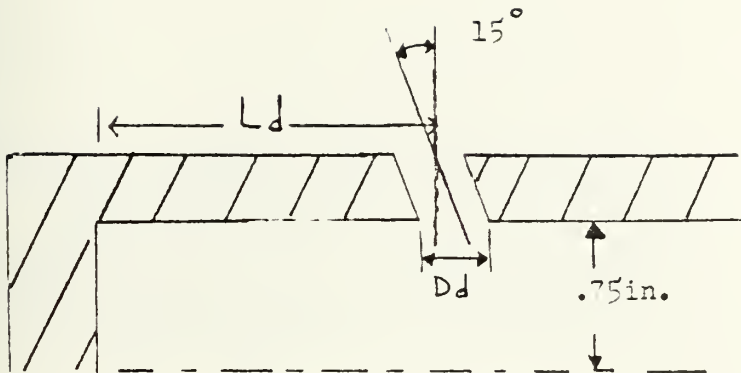


Figure 3. Photograph of Ramjet Motor Assembly with Shortened Aft Mixing Chamber.



$L_d = 2.1\text{ in.}$
 $D_d = 0.354\text{ in.}$

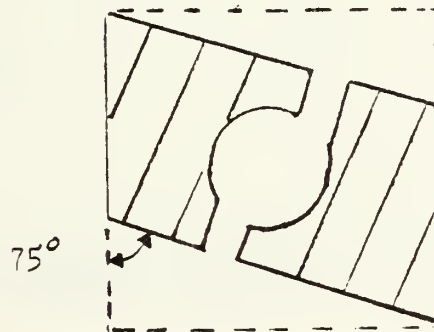
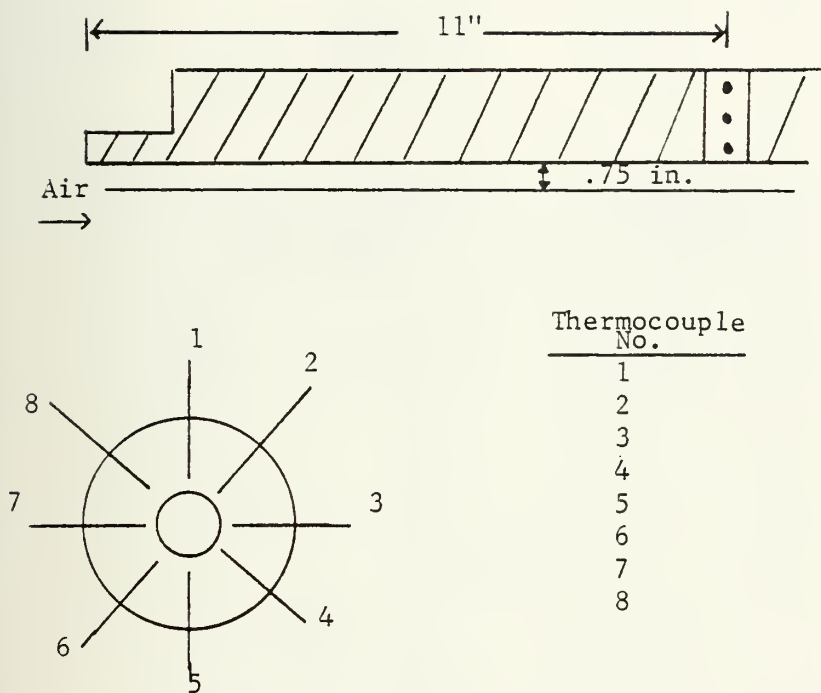


Figure 4. Schematic of Cylindrically Perforated Fuel Grain with Twin Side-Dump/ Dome Inlets.



Thermocouple
No.

Gage

Distance
from
Inside
Wall (in.)

1
2
3
4
5
6
7
8

30
30
30
30
36
36
36
36

0.02
0.10
0.18
0.25
0.02
0.10
0.18
0.25

Figure 5. Schematic of Cylindrically Perforated Fuel Grain with Imbedded Thermocouples.

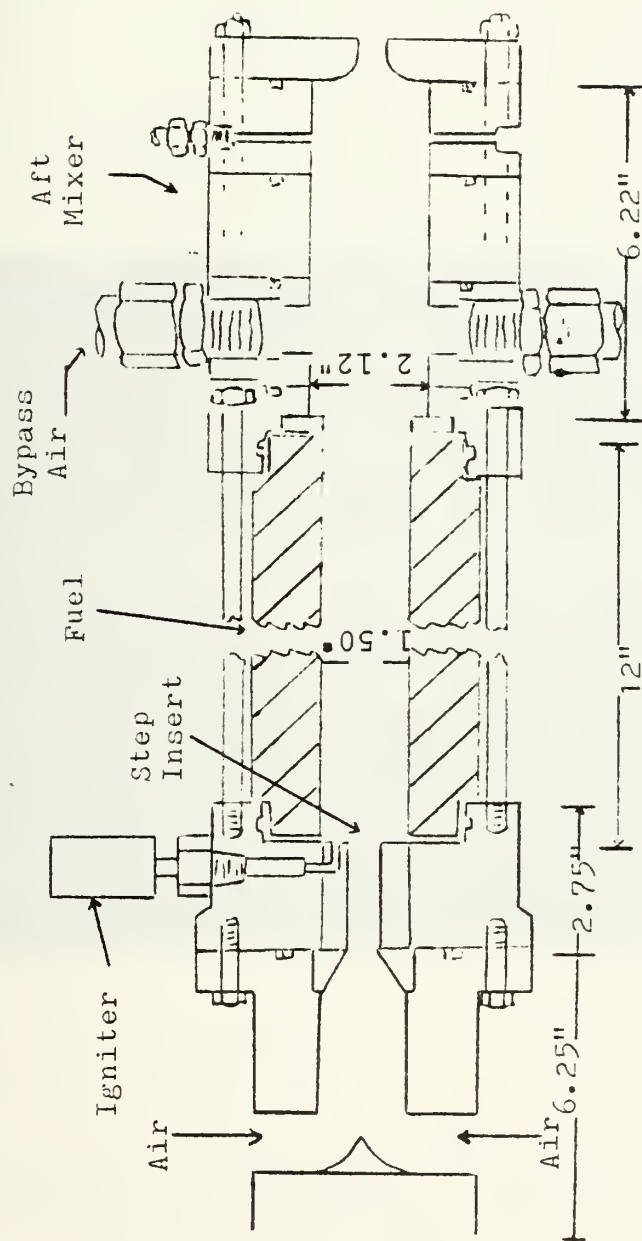


Figure 6. Schematic of Solid Fuel Ramjet Assembly

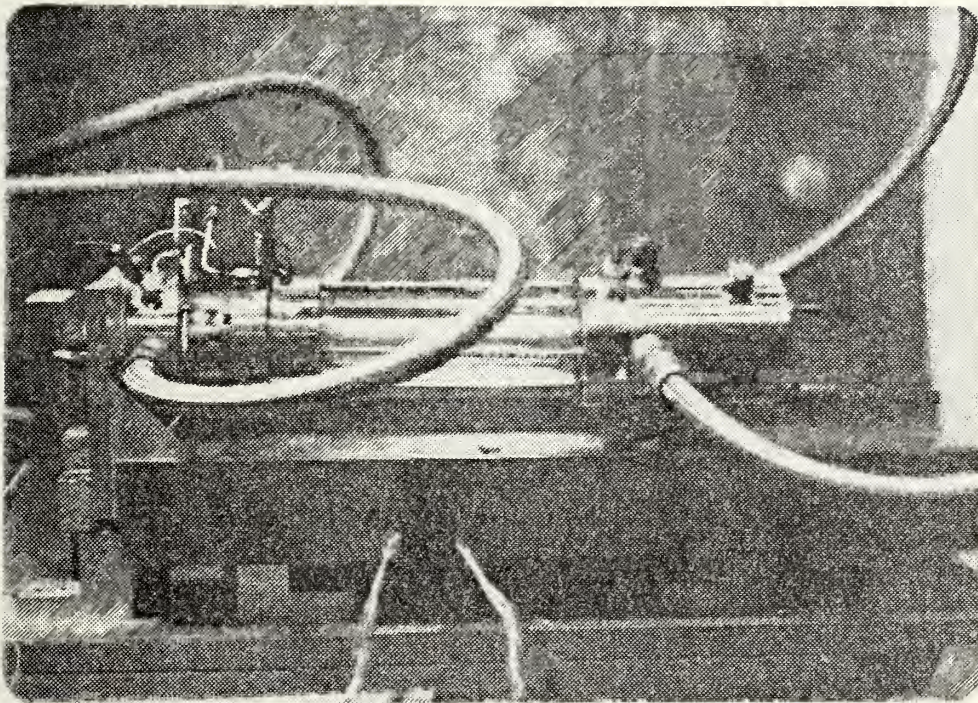


Figure 7. Photograph of Solid Fuel Ramjet Assembly

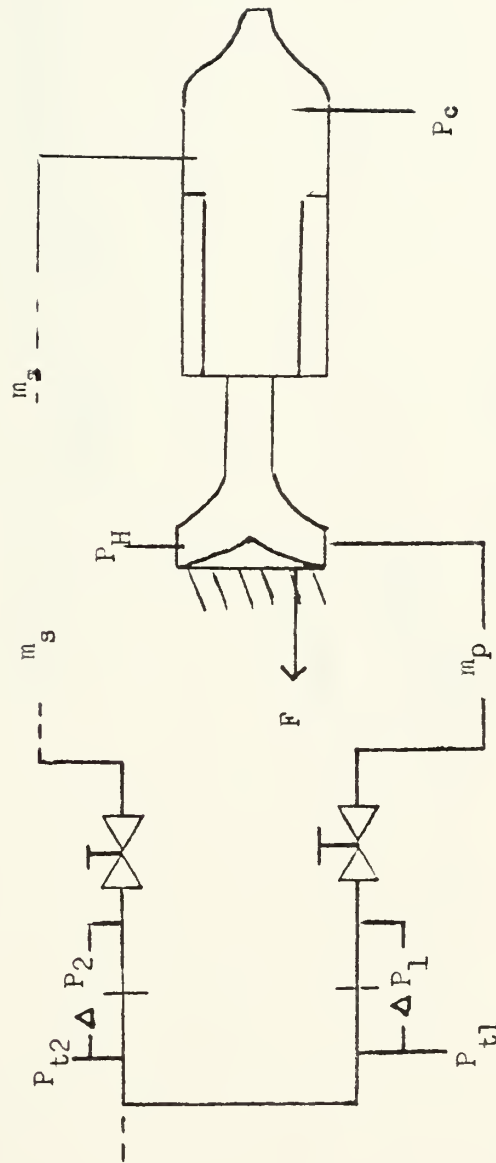
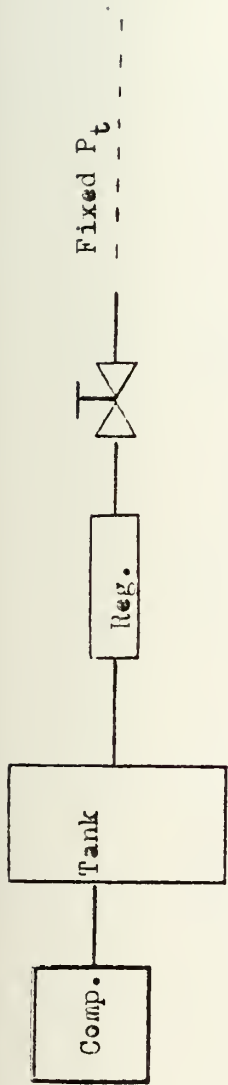


Figure 8. Schematic of Air Supply System

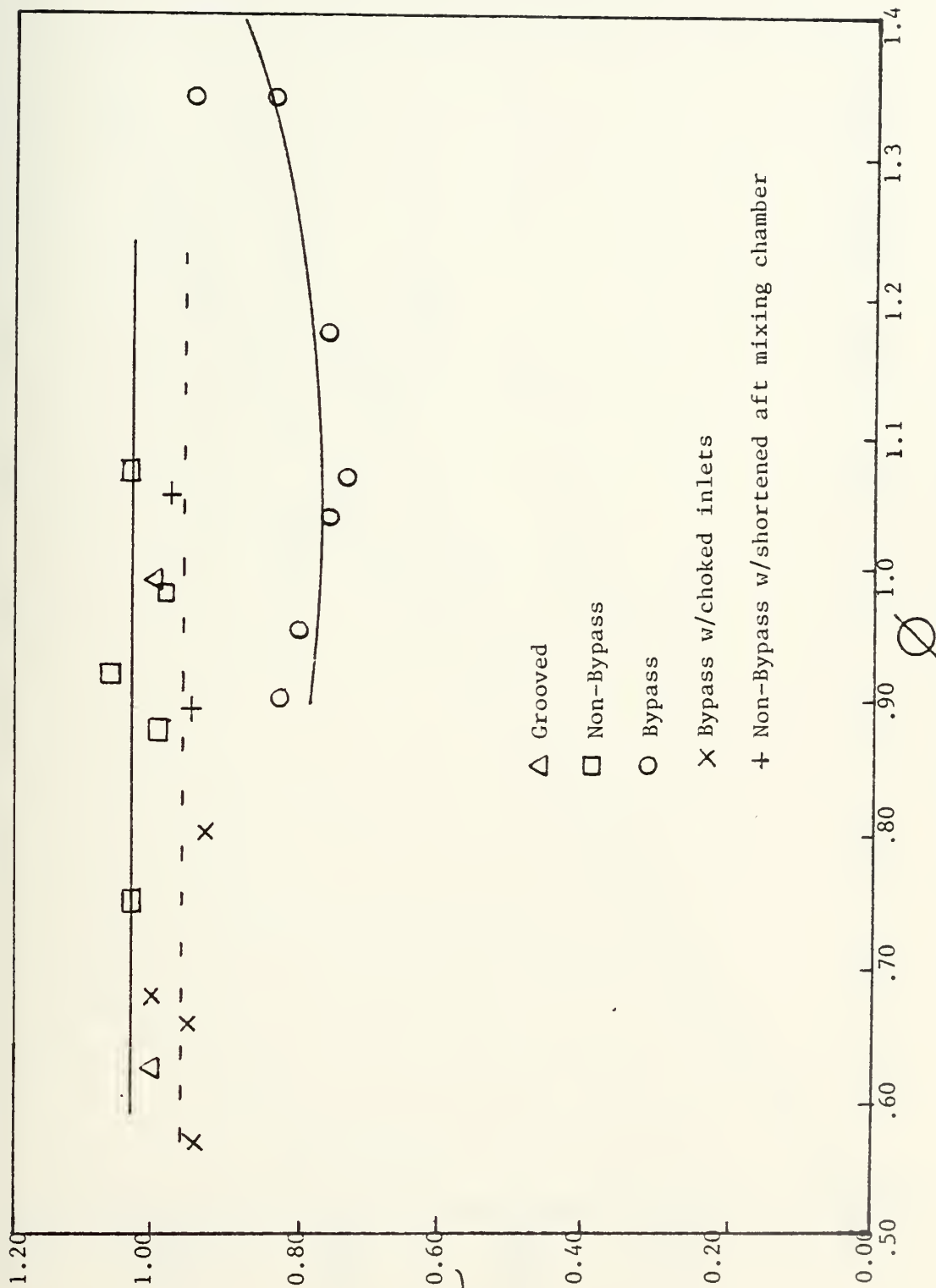
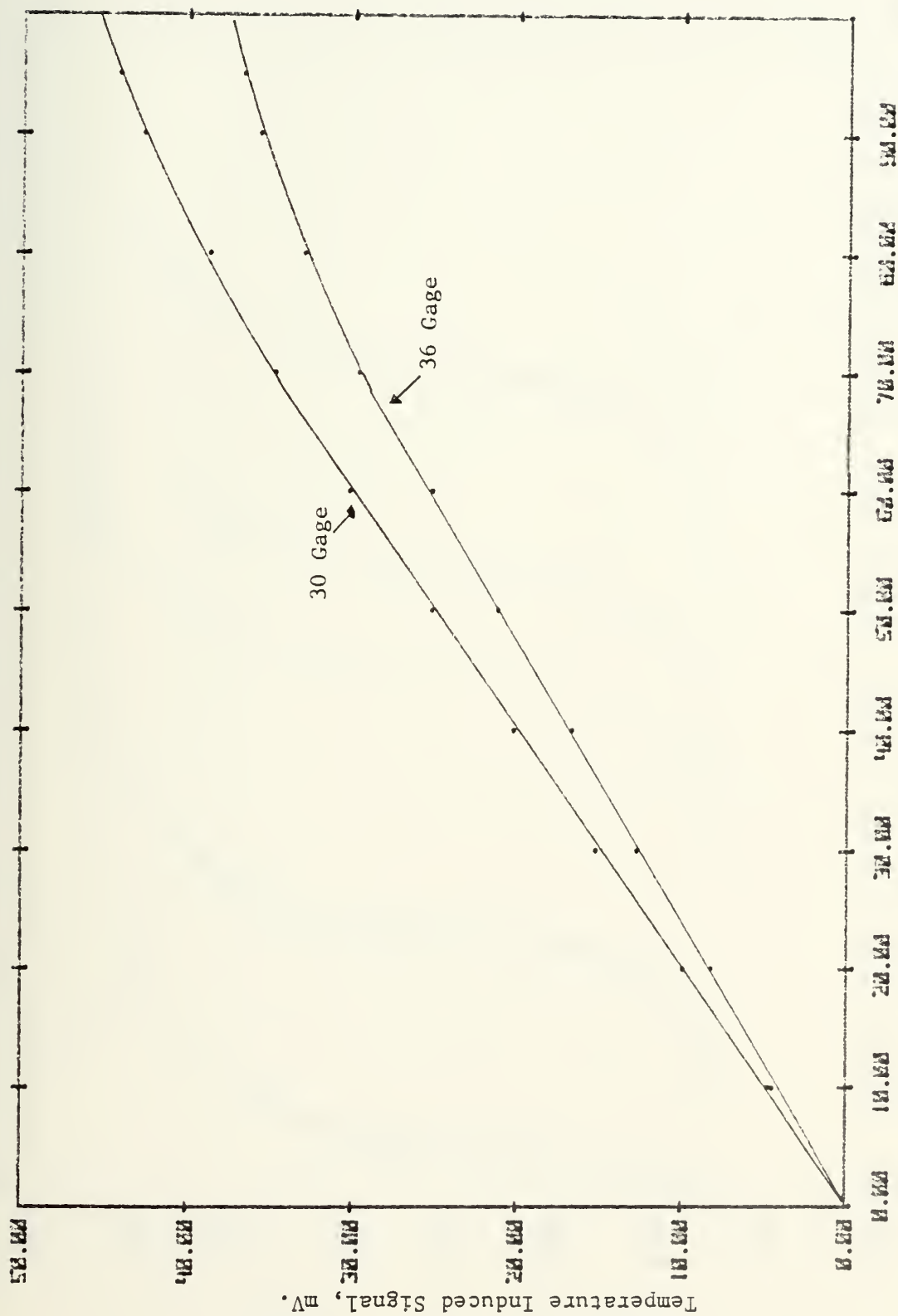
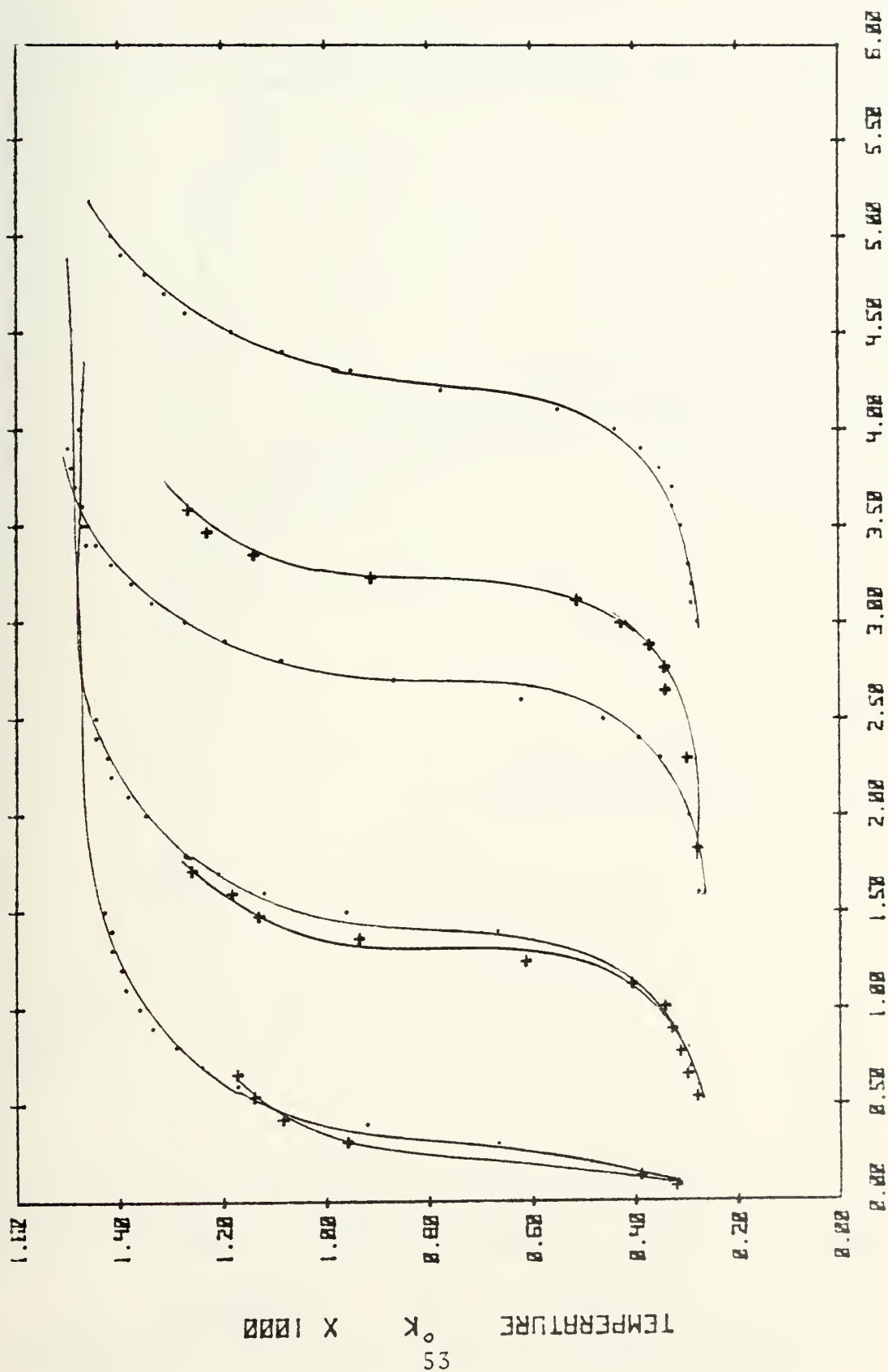


Figure 9. Combustion Efficiency vs. Mixture Ratio



Galvanometer Deflection, mm
Figure 10. Thermocouple Calibration Curves



TIME SECONDS X 10

Figure 11. Temperature vs. Time for Experiment No. 20

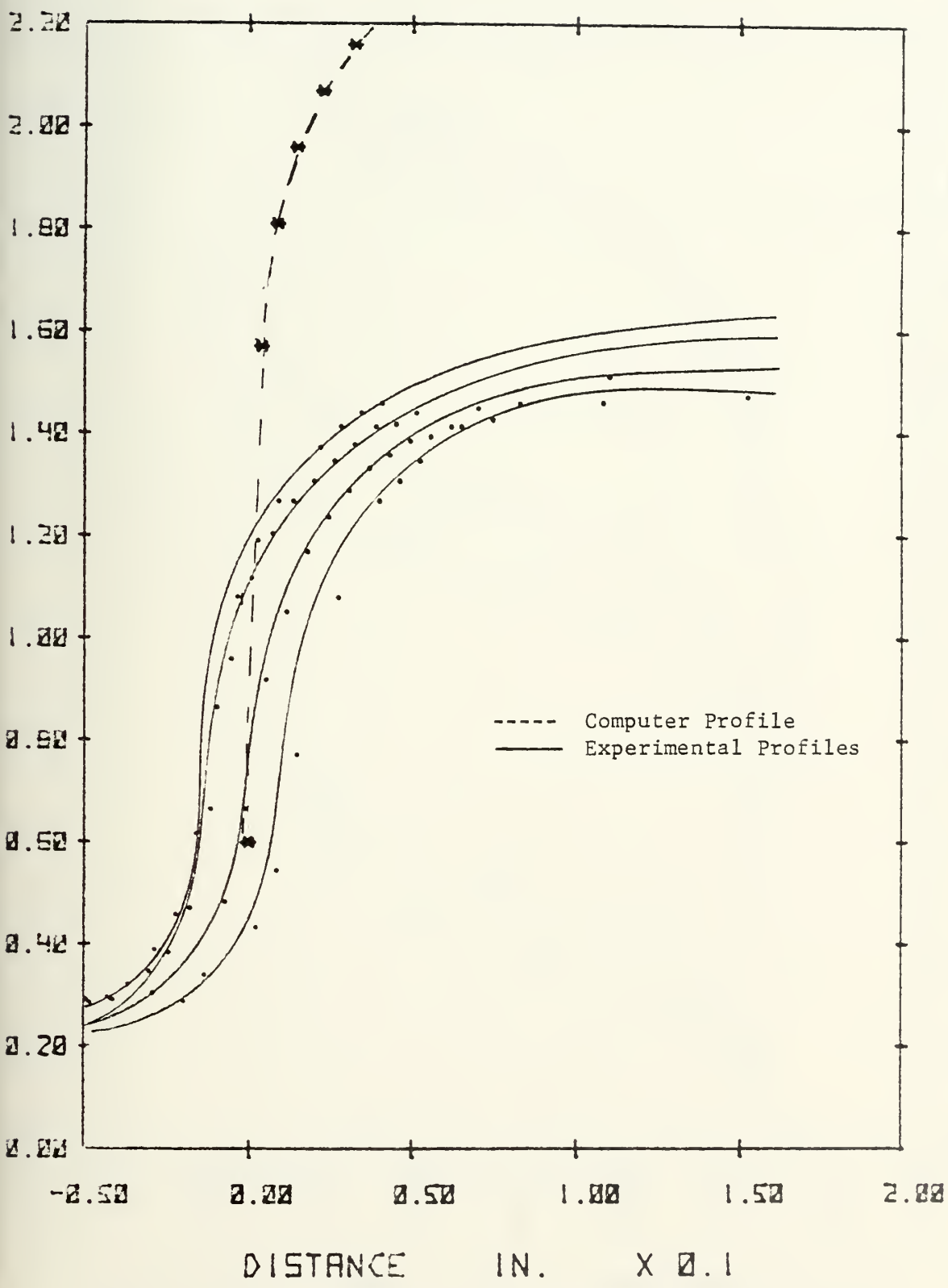
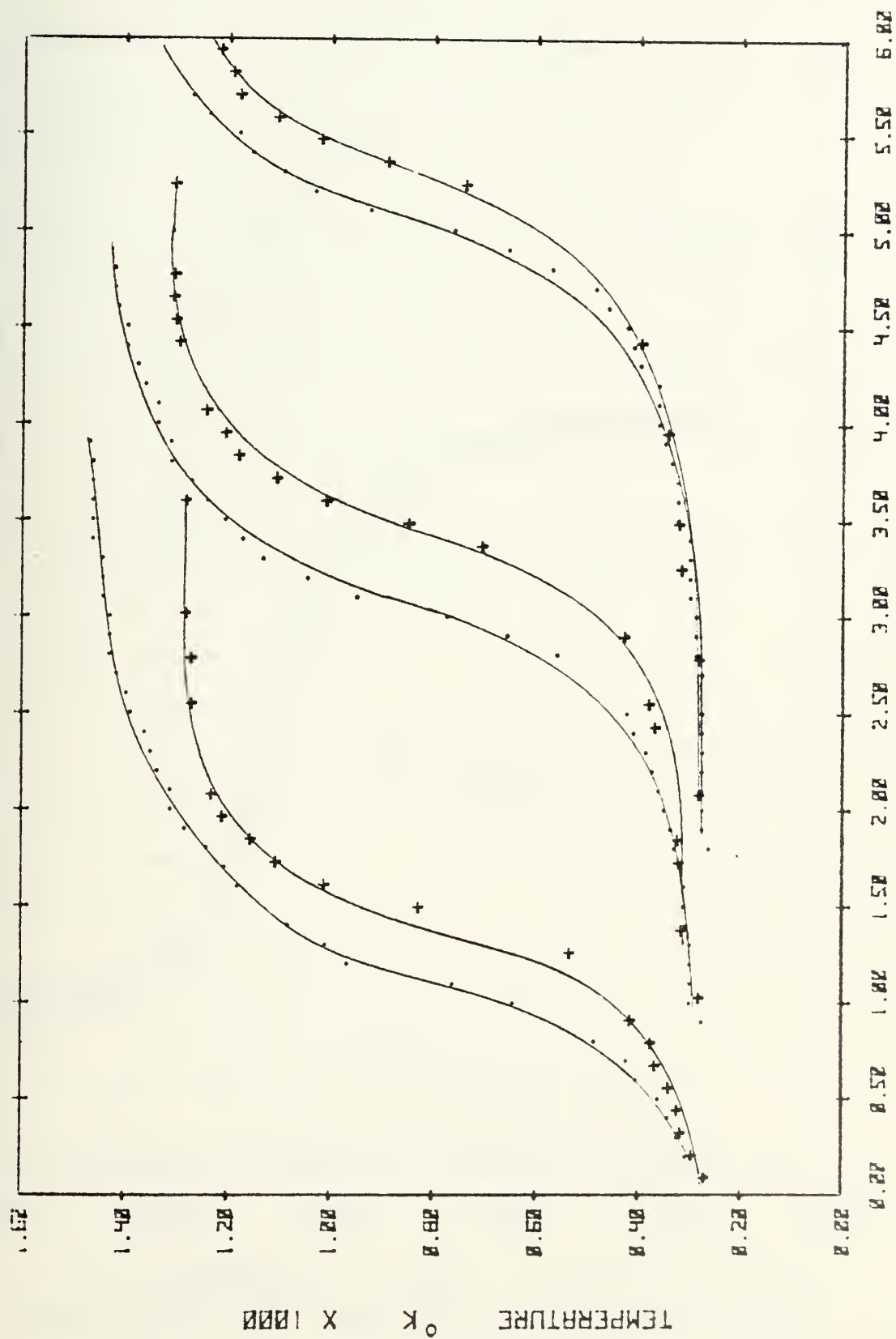


Figure 12. Radial Temperature Profiles for Experiment No. 20



TIME SECONDS X 10

Figure 13. Temperature vs. Time for Experiment No. 19

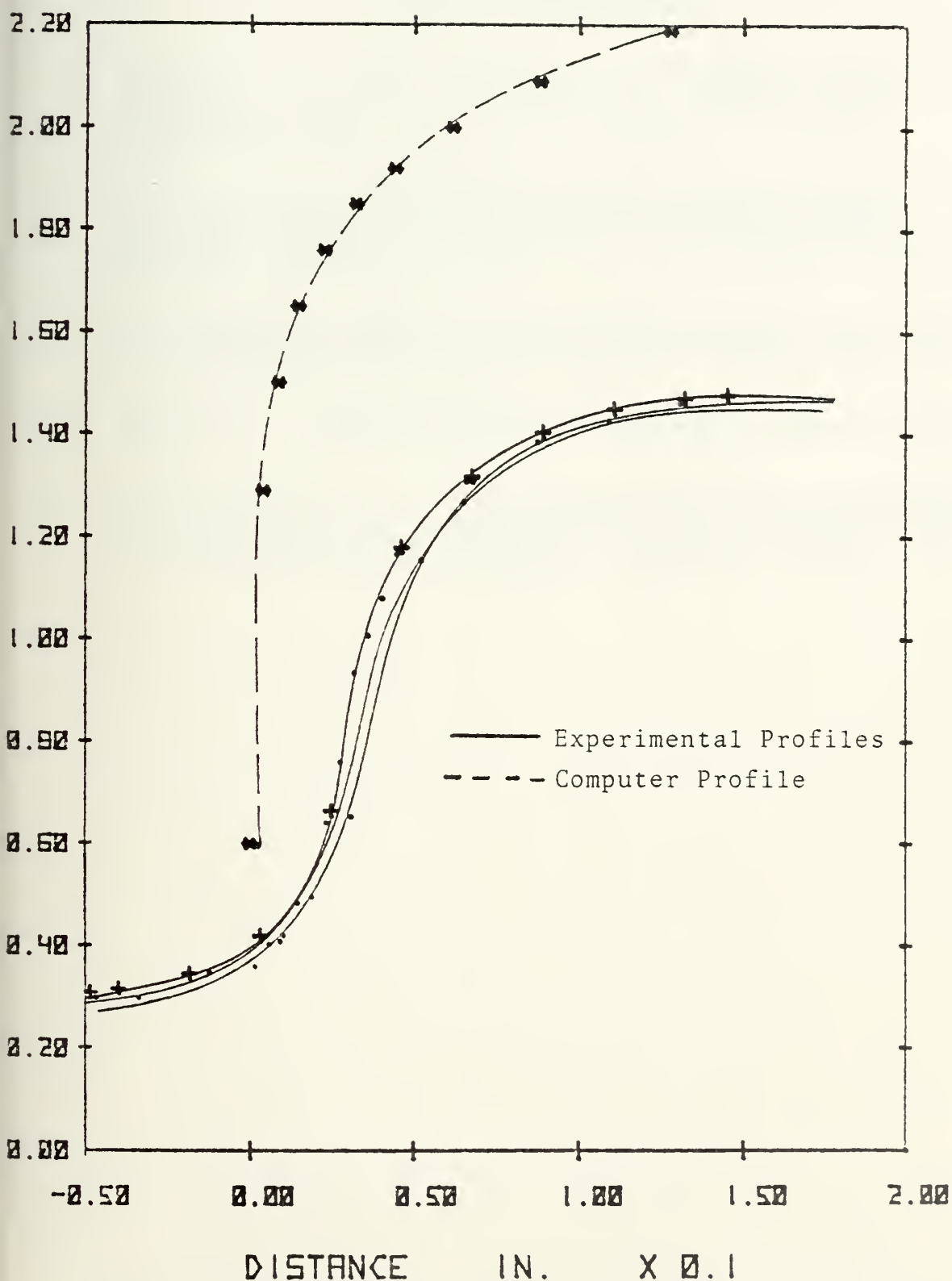


Figure 14. Radial Temperature Profiles for Experiment No. 19

LIST OF REFERENCES

1. Kinroth, G. D. and Anderson, W. R., Ramjet Design Handbook, Chemical Propulsion Information Agency Publication 319, 1980.
2. Scott, W. E., An Investigation of the Reacting and Non-Reacting Flow Characteristics of Solid Fuel Ramjets, Master's Thesis, Naval Postgraduate School, Monterey, California, 1979.
3. Fluid Meters, Their Theory and Application, Report of the American Society of Mechanical Engineers Research Committee on Fluid Meters, 1971.
4. Mironer, A., Engineering Fluid Mechanics, McGraw-Hill, 1979.
5. Metochianakis, M., An Investigation of the Combustion Behavior of Solid Fuel Ramjets, Master's Thesis, Naval Postgraduate School, Monterey, California, 1980.

INITIAL DISTRIBUTION LIST

	No. Copies
1. Defense Technical Information Center Cameron Station Alexandria, Virginia 22314	2
2. Library, Code 0142 Naval Postgraduate School Monterey, California 93940	2
3. Department Chairman, Code 67 Department of Aeronautics Naval Postgraduate School Monterey, California 93940	1
4. Professor D. W. Netzer Code 67Nt Department of Aeronautics Naval Postgraduate School Monterey, California 93940	2
5. Mr. Uri Katz Department 48 Post Office Box 2250 Haifa, Israel	2
6. LCDR William V. Goodwin 51 Semmes Court La Plata, Maryland 20646	2

Thesis
G57335 Goodwin
c.1
An investigation of
the combustion process
in solid fuel ramjets.
JUN 19 65
29498

Thesis
G57335 Goodwin
c.1
An investigation of
the combustion process
in solid fuel ramjets.

thesG57335

An investigation of the combustion proce



3 2768 002 13117 9

DUDLEY KNOX LIBRARY